VAPOR-BUBBLE GROWTH AT THE LOWER GENERATRIX OF HORIZONTAL TUBES

V. D. Chaika

UDC 536.248.2

The results of cinematographic investigation of vapor-bubble growth in the boiling of water at horizontal tubes are given. Theoretical and experimental data on bubble growth at the lower generatrix of horizontal tubes are compared.

Vapor-bubble growth is investigated in the boiling of distilled water at elements of horizontal copper tubes of diameter 10, 16, 24, 34, and 70 mm. The process is recorded by means of cine cameras in two projections simultaneously: with specific thermal loads of 20 and 40 kW/m^2 and a saturation pressure of 100 kPa.

The basic characteristics of vapor-bubble growth – the vapor volume; the shape of the vapor volume; the growth rate; the velocity of bubble flow around the tube on emersion – are studied in analyzing the cine recordings. The volume of the vapor bubble is determined as the volume of the ellipsoid of revolution. In the case when the form of the vapor bubble is not an ellipsoid of revolution, the volume is calculated by the Simpson formula. The vapor-bubble radius is determined from the vapor volume. The greatest error in determining the vapor volume by the given method is 12%.

The characteristics of vapor-bubble growth are calculated using a computer [1].

Earlier [2], it was established that bubble boiling begins with the nucleation of vapor bubbles at the lower generatrix of horizontal tubes and the basic volume of vapor phase leaves the heating surface in the lower part of the tubes. Vapor formation in the upper part of the tubes is analogous to water boiling at horizontal plane heating surfaces.

The literature has no data on vapor-bubble growth at the lower generatrix of a horizontal tube, and so this growth is studied in the present work.

Vapor-bubble growth at the lower generatrix of a horizontal tube may be divided into the following stages: 1) nucleation; 2) growth up to breakaway from the nucleation center; 3) breakaway from the nucleation center; 4) flow around the tube surface in emersion; 5) breakaway from the tube surface [2].

The development of the vapor bubble is shown schematically in Fig. 1.

In the experimental conditions, the first stage of growth is not studied. At the beginning of the second stage, vapor-bubble growth occurs in the same way as on a horizontal plane heating surface. The bubble takes the form of a sphere and expands without deformation, reaching a radial dimension of 1.25 mm. The limiting angles (frontal Θ_0^0 and rear Θ_1^0) are approximately 20-48°. Continuing to develop on both sides of the tube (as seen from the end of the tube), it is deformed, coming to resemble an ellipsoid of revolution, and spreads over the tube surface. Its base takes the form of an ellipse, the major axis of which coincides with the tube axis. According to the cine recordings, the base surface of the vapor bubble and the deformation of its volume increase with increase in diameter of the horizontal tube, and reach maximum values in the third stage of growth.

The third stage of growth begins with unidirectional motion of the frontal phase interface over the tube perimeter. The limiting frontal angle decreases here ($\Theta_0 \to 0$) and the rear angle increases ($\Theta_1 \to 180°$). These changes are determined by the diameter of the horizontal tube. The third stage of vapor-bubble growth ends when its rear boundary passes beyond the limits of its lower generatrix.

Far-East Technical Institute of the Fishing Industry and Agriculture, Vladivostok.
Translated from Inzhenerno-Fizicheskii Zhurnal, Vol. 52, No. 1, pp. 66-73, January, 1987. Original article submitted October 23, 1985.

 0022-0841/87/5201-0052$12.50

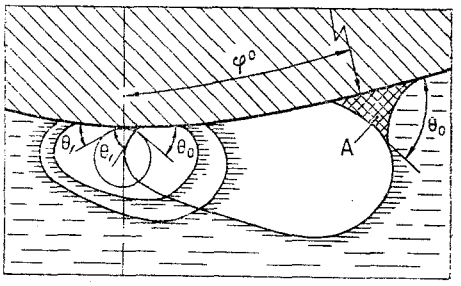

Fig. 1. Vapor-bubble growth at the lower generatrix of a horizontal tube: A, wedge-shaped underlayer; φ^0, azimuth of frontal boundary of vapor bubble; Θ_0 and Θ_1, frontal and rear angles, respectively.

The vapor-bubble development at the lower generatrix of a horizontal tube is monitored from the azimuth of its frontal boundary (φ^0). The azimuth of the point of bubble breakaway from the nucleation center at the lower generatrix for tubes of the given diameters is 12-18°.

When the rear boundary of the vapor bubble passes beyond the limits of the lower generatrix, its base shrinks. The rear boundary of the base contracts toward the frontal part, as it were. Transition from the instant of breakaway to the onset of flow around the tube occurs with steady motion of the rear boundary.

The fourth stage of growth – the flow of the vapor bubble around the tube surface as it floats upward – is analogous, to a certain degree, to the third stage of growth. However, the increments of the vapor bubble in the third stage develop more intensively.

Analysis of cine recordings allow an analogy to be drawn between the development of the vapor volume at the lower generatrix and an inverse process of condensate-drop flow from the surface of a horizontal tube.

On approaching the fifth stage of bubble growth, its flow velocity around the tube surface as it rises decreases; its base surface is sharply constricted here and breakaway from the tube surface is seen to be accompanied by breakaway of the wall layers of liquid and their motion toward the bubble base.

In boiling on horizontal plane heating surfaces, the rate of vapor-bubble growth and its shape, according to numerous investigations, are determined by the Jacob number. Thus, in conditions of atmospheric pressure, with Ja = 13.9, bubbles of spherical form are seen; at Ja = 23.3, flattened bubbles; at Ja = 32.2, hemispherical bubbles [3].

Cine recordings of vapor-bubble growth at the lower part of a tube of diameter 70 mm are shown in Fig. 2; it is seen that at Ja = 12.2 the bubble deformation is greater than at a tube diameter of 10 mm with Ja = 27 and the microlayer area is a maximum.

At the lower generatrix of the horizontal tube, the lift force is directed upward and, compressing the vapor bubble, it increases the bubble deformation. Hence, whereas on a plane horizontal heating surface the shape and size of the vapor bubble, the microlayer geometry, and the velocity of its frontal broundary are characterized by the Jacob number, on the lower part of a horizontal tube these characteristics are determined by a set of thermal and hydrodynamic conditions: the overheating of the wall over the tube perimeter, the temperature field in the liquid around the heated tube, and the magnitude and direction of the mean-velocity vector of the frontal phase interface relative to the gravitational vector.

According to the data of the cine recordings, the radial dimension of the vapor-bubble dimension at the instant of breakaway from the heating surface depends on the horizontal-tube diameter for the specified conditions. This dependence takes the form

$$R = 0{,}73\Phi_{\text{н}}^{0{,}84}. \quad (1)$$

Increase in diameter of the horizontal tube is evidently accompanied by increase in the influence of the hydrodynamic conditions on the rate of vapor-bubble growth and its radial dimension at breakaway from the tube surface. In the course of the whole growth period on the horizontal tube, the vapor bubble increases continuously in volume. The radial dimension of the vapor bubble in its period of growth on a horizontal plane heating surface conforms to the law

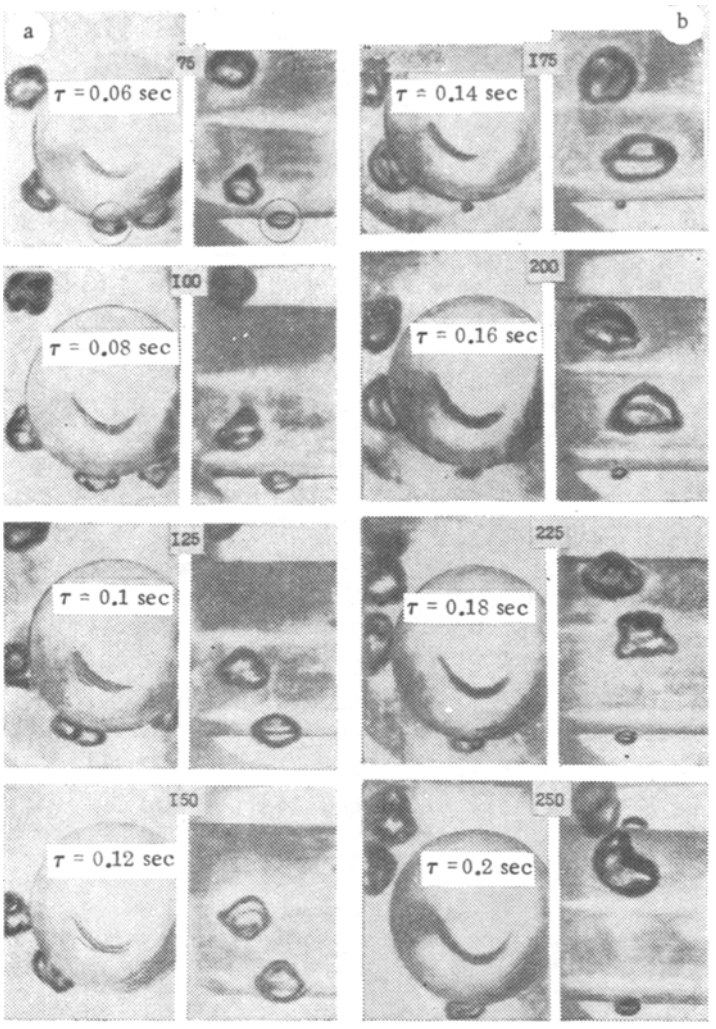

Fig. 2. Cine recordings of vapor-bubble growth at a tube of diameter 70 mm with q = 20 kW/m^2 and P = 100 kPa: a, b) profile and frontal projections, respectively; τ, growth time from the instant of vapor bubble nucleation; 75, 100, ..., 250, frame numbers; W = 1250 frame/sec, speed of cine film.

$$R = A\tau^n, \tag{2}$$

where A is a coefficient proportional to $\Delta T_w = T_w - T_H$. According to literature data, the exponent n depends on the material and state of the heating surface and changes with vapor-bubble growth from 1/2 to 1/4 [3-5].

Analysis of the results of investigating the change in vapor-bubble radius over time as it grows on the lower generatrix of horizontal tubes of diameter 10 and 70 mm (Figs. 3 and 4) shows that each stage in vapor-bubble growth corresponds to a definite rate of increase in its radial dimension. In Figs. 3 and 4, these growth stages are denoted by curves a-d, respectively.

In the volume of superheated liquid, the vapor-bubble growth is regulated by such effects as the intensity of heat supply from external superheated layers, the magnitude of the inertial reaction, and the viscous drag of the liquid. The determining influence of each of these effects on the vapor-bubble growth depends on the thermal and hydrodynamic conditions around the interphase boundary and the physical properties of the medium [6]. As follows from the concepts regarding the mechanism of bubble boiling outlined in [6], in the nucleation of a vapor bubble at the lower generatrix of a horizontal tube, the rate of increase in its radial dimension is supplemented by the following components: evaporation of the microlayer and evaporation of the wedge-shaped underlayer at its base (Fig. 1).

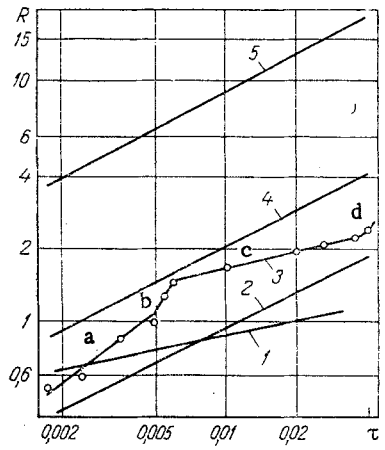

Fig. 3

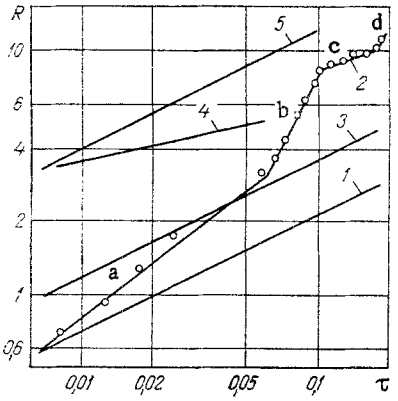

Fig. 4

Fig. 3. Dependence of the vapor-bubble radius on the time at a tube of diameter 10 mm when q = 40 kW/m^2: 1) Eq. (5); 2) Eq. (4); 3) experiment; 4) Eq. (3); 5) Eq. (8); a-d) stages in vapor-bubble growth: up to breakaway from the nucleation center at the lower generatrix; breakaway from the nucleation center; flow around the tube on emersion; breakaway from the tube surface. R, mm; τ, sec.

Fig. 4. Dependence of the vapor-bubble radius on the time at a tube of diameter 70 mm when q = 40 kW/m^2: 1) Eq. (4); 2) experiment; 3) Eq. (3); 4) Eq. (5); 5) Eq. (8); a-d) as in Fig. 3.

In real conditions, of course, the increase in radial dimension of the vapor bubble at a horizontal tube is regulated, after a certain time interval, by all the above-noted components.

Analysis of the known models of vapor-bubble growth shows that each model is only applicable for a single limiting case, i.e., when the evaporation of liquid in the vapor bubble is controlled by one such process.

Below, the known models of vapor-bubble growth are compared with experimental data, with the aim of:

1) establishing the applicability of the known models of vapor-bubble growth to its growth at the lower part of a horizontal tube;

2) determining the contribution of each component in liquid evaporation in a vapor bubble;

3) elucidating the reasons for possible discrepancy between theoretical and experimental data.

The Cooper formula

$$R_{\text{M}} = 2{,}5\,\text{Ja}\,\sqrt{\nu\tau}/\text{Pr} \qquad (3)$$

is applicable for the determination of the radial dimension of the vapor bubble as it grows on a horizontal plane heating surface in the case of predominant evaporation of the microlayer under its base. However, calculation by this formula gives an overestimate for the whole period of bubble growth at a tube of diameter 10 mm (Fig. 3, curve 4).

For a tube of diameter 70 mm, the data from Eq. (3) coincide with the experimental results only partially for the second stage of vapor-bubble growth (Fig. 4, curve 3). The theoretical curve from Eq. (3) passes above the experimental data for the second stage of bubble growth, intersecting the curve approximating the experimental results at the end of this stage. For the other stages of bubble growth, these discrepancies are qualitatively and quantitatively different and Eq. (3) gives underestimates.

Analysis of Eq. (3) shows that it does not include such characteristics of the microlayer as its area and the thickness over its perimeter, and takes no account of the influence of hydrodynamic conditions on the evaporation rate of the liquid in the vapor bubble.

At a horizontal plane heating surface in the case of predominant heat supply through the wedge-shaped underlayer, the bubble dimension is determined from the Labuntsov formula

$$R_U = \sqrt{2\beta \frac{\lambda \Delta T_w \tau}{r\rho''}}, \quad (4)$$

where $\beta = 10$.

Comparison of the theoretical data from Eq. (4) with experimental data for the second stage of vapor-bubble growth indicates that the experimental data coincide with the theoretical data for tubes of diameter 10 and 70 mm only for a short time interval (Fig. 3, curve 2; Fig. 4, curve 1). For other stages of bubble growth, the experimental data exceed the theoretical data, despite the developed wedge-shaped underlayer at its base.

The distinguishing feature of vapor-bubble growth at the lower part of the horizontal tube is the developed area of the bubble base. Thus, at a tube of diameter 10 mm, the greatest area of the bubble base is 3.4 mm^2; at a tube of diameter 70 mm, the corresponding value is 480 mm^2.

In calculating the rate of liquid evaporation from a microlayer into the vapor bubble, it was assumed in [7] that the heat influx to the interphase surface of the bubble is by heat conduction and the formula proposed was

$$Q_M = \int_0^{\tau} \int_0^{F_M} \frac{\lambda \Delta T_w}{\delta_M} dF_M d\tau, \quad (5)$$

where F_M is the base surface of the (greatest) vapor bubble.

The thickness of the liquid microlayer under the vapor-bubble base is determined from the Cooper formula

$$\delta_M = 0{,}8\sqrt{\nu\tau}. \quad (6)$$

The vapor-bubble radius for any time in the growth process is

$$R_{M^*} = \sqrt[3]{\frac{Q_M(\tau)}{4/3\pi r\rho''}}. \quad (7)$$

The area of the vapor-bubble base is determined in analyzing the cine recordings by the well-known method [1].

The theoretical results from Eq. (5) and the experimental data on vapor-bubble growth do not coincide (Fig. 3, curve 1; Fig. 4, curve 4); the quantitative character of this discrepancy changes in the course of the whole period of vapor-bubble growth. For example, for a tube of diameter 70 mm, the curve plotted from theoretical data lies above the experimental results for the second stage of growth and for the first half of the third stage of growth. In the remainder of the growth period, the increase in radial dimension of the vapor bubble over time exceeds the theoretical data on the radial dimension from Eq. (5).

At a tube of diameter 10 mm, the discrepancy between the theoretical and experimental data for the first half of the second stage of vapor-bubble growth reverses sign, and an underestimate is obtained. Only qualitative agreement of the data of this model for vapor-bubble growth in bubble flow around the tube surface is observed. In this case, the influence of turbulent heat conduction on the intensity of liquid evaporation in the vapor bubble probably appears.

In the evaporation of superheated liquid layers surrounding a vapor bubble, the conditions of bubble growth are approximated by the well-known relation [8]

$$R_L = 2\sqrt{3/\pi}\,[1 + 1/2\,(\pi/6\,\mathrm{Ja})^{2/3} + \pi/6\,\mathrm{Ja}]^{1/2}\,\mathrm{Ja}\sqrt{a\tau}. \quad (8)$$

Comparison of experimental data for the second stage of growth with theoretical data from Eq. (8) gives the greatest discrepancies. Data from Eq. (8) exceed the experimental results by a factor of 3-7 (Fig. 3; Fig. 4, curve 5); the greatest discrepancy is found with a tube diameter of 10 mm.

The basic parameter of Eq. (8) is the Jacob number. It includes the quantity ΔT_w, whose value is taken to be constant and equal to the wall overheating at the moment of vapor-bubble nucleation. However, it is known that the temperature of the superheated liquid layers sur-

rounding the vapor bubble decreases over time, which is not taken into account by the Jacob number in Eq. (8).

Thus, it is evident from cine recordings of water boiling at atmosphere pressure that the diameter of the horizontal tube influences the linear dimensions of the vapor bubble, the shape of the vapor volume, and the surface of its base over time and regulates the velocity of the frontal boundary of the bubble, i.e., the dynamics of its growth.

NOTATION

A, numerical coefficient; a, thermal diffusivity, m^2/sec; C, specific heat of water, kJ/kg·K; d_H, tube diameter, m; F_M, area of microlayer, m^2; g, acceleration due to gravity; m/sec^2; n, exponent; P, saturation pressure; kPa; R, radius of vapor bubble, m; R_M, R_L, R_U, radial dimension of vapor bubble in liquid evaporation from a microlayer, the surrounding liquid layers, and the wedge-shaped underlayer, m; r, heat of vaporization, kJ/kg; T_W, wall temperature, K; T_H, saturation temperature; $\Delta T_W = T_W - T_H$, temperature difference, °K; β, numerical coefficient; δ_M, microlayer thickness; Θ^0, limiting angle, deg; λ, thermal conductivity, W/m·K: ν, kinematic viscosity; m^2/sec; $\pi = 3.142$; ρ', ρ'', density of water and vapor, kg/m^3; σ, surface tension, N/m; τ, time of vapor-bubble growth, sec; φ^0, central angle of vapor-bubble displacement over the tube perimeter, deg; $Pr = \nu/a$, Prandtl number; $Ja = C\rho'\Delta T_W/r\rho''$, Jacob number; $\ell = \sqrt{\sigma/g(\rho' - \rho'')}$, Laplace constant, m; $\Phi_H = 1 + [(d_H/\ell) - 1] \exp(-10^{-3} d_H/\ell)$, parameter taking account of the influence of the horizontal-tube diameter.

LITERATURE CITED

1. Yu. V. Yakubovskii, B. Ya. Karastelev, V. D. Chaika, et al., Operating Processes in Marine Water-Distillation Units and Research Methods. Educational Text [in Russian], Vladivostok (1976).
2. V. D. Chaika, Some Features of the Dynamics of Vapor-Bubble Growth in the Boiling of Water at Horizontal Tubes in Conditions of Atmospheric and Reduced Pressure. Paper No. rp-D82 Deposited at TsNIITÉIRKh [in Russian], Vladivostok (1982).
3. N. B. Hospeti and R. B. Mesler, AIChEI, 15, No. 2, 214-220 (1969).
4. P. Grifith, Trans. ASME, 80, 721-726 (1958).
5. A. P. Hatton and I. S. Hall, in: Proceedings of the Third International Heat Transfer Conference, Chicago (1966); AIChEI, 4, No. 4, 24-37 (1966).
6. D. A. Labuntsov, Heat Transfer and Physical Gas Dynamics [in Russian], Moscow (1974), pp. 98-115.
7. V. I. Subbotin, D. N. Sorokin, and A. A. Tsyganov, Izv. Akad. Nauk SSSR, Energ. Transp., No. 4, 93-101 (1976).
8. D. A. Labuntsov, B. A. Kol'chugin, V. S. Golovich, et al., Teplofiz. Vys. Temp., 2, No. 3, 446-453 (1964).